Pattern formation and competition in nonlinear optical systems with two-dimensional feedback

M. A. Vorontsov and W. J. Firth
International Laser Centre, Moscow State University, 199899 Moscow, Russia;
New Mexico State University, Las Cruces, New Mexico 88003;
and Department of Physics and Applied Physics, University of Strathclyde, Glasgow G4 0NG, Scotland
(Received 3 August 1993)

Nonlinear optical systems using a Kerr slice and two-dimensional feedback are analyzed. A Neumann-series approach is used to study pattern formation. We show that interactions between spatial modes (rolls) occur in the form of "winner-takes-all" dynamics and cause formation of hexagon patterns.

PACS number(s): 42.65.−k

I. INTRODUCTION

It seems the time of the plane-wave approximation is ending in nonlinear optics. This fruitful approach has allowed us to factorize spatial and temporal variables and analyze effects separately. We now realize that even more interesting and extraordinary phenomena occur when time and space are mixed together. Even in quite simple nonlinear optical systems [Kerr slice with a feedback mirror [1–4], mirrorless counterpropagating beams [5–7], nonlinear passive resonator or interferometer [8,9], two-dimensional (2D) feedback system with long-range interactions [10,11]] it is possible to obtain a large variety of dynamic regimes: bistability and multistability, dissipative structures, traveling and switching waves, optical vortices, hexagons and other polygons, bright and dark solitons, and related diffractive patterns [12,13], [14–16], etc. Very often several different regimes of spatiotemporal self-organization coexist in the same system and under the same or similar parameter values [17,18].

Here our concern is with nonlinear phenomena where interactions between nonlinear modes (patterns, structures, images, etc.) play important or decisive roles. In this respect the more traditional and convenient approach to the study of nonlinear dynamics based on linear stability analysis is insufficient. We need to use something more complicated; for example, multiple-scale analysis (MSA) [19]. But for this case instead of one or two nonlinear equations we would obtain a series of rather complicated partial differential equations [4]. It is some consolation that the Ginzburg-Landau equation frequently appears in a second-order calculation [19,20]. As far as higher-order equations are concerned, it has been remarked that they involve lengthy algebra, and to use a simpler but less rigorous approach is more convenient [4]. We follow this latter recommendation from the beginning.

In this paper we attempt to analyze and explain the pattern formation process. During this process a continuous infinity of candidate modes collapse, through mode-mode competition, to a small number of surviving modes constituting the fully formed set.

Here we consider the simplest nonlinear optical systems where cooperative and competitive dynamics take place. The basic models are presented in Fig. 1, namely a thin antireflective slice of Kerr medium with a feedback mirror [Fig. 1(a)] [21,1,2] and a system consisting of a thin Kerr-like medium with reflection and external feedback [Fig. 1(b)]. An example of the latter is an optical system with 2D feedback and a liquid crystal light valve (LCLV) used as a model of a Kerr slice [10,22]. Under certain conditions both systems can be similarly described [23].

Our approach is based on the following observations.

(1) A finite number of more active interacting "modes" play an important role in the formation stage of nonlinear spatial patterns. We use this observation to reduce the original nonlinear partial differential equations to a system of equations for the active mode amplitudes. The animate body of the nonlinear dynamics is shaped by this system of equations.

(2) Formation of nonlinear patterns due to interaction

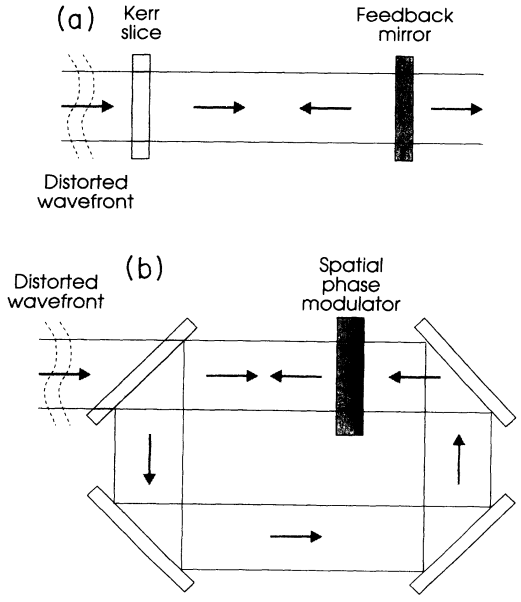

FIG. 1. Two optical systems which are equivalent in terms of the present analysis: (a) Kerr slice with feedback mirror; (b) nonlinear passive resonator controlled by a spatial phase modulator driven by light through a 2D feedback loop.

between modes occurs with small mode amplitude values in the vicinity of the bifurcation point where stability is lost. We assume that the most interesting features of the pattern that develops arise in this vicinity. This allows us to correct the linear stability analysis and keep the most important intermode interactions. The question is, how do we make this correction?

It would seem natural to make the typical expansion of the nonlinear equations in a Taylor series and keep only the terms of the zero, first, second, and, given enough patience, third order [20,4]. However, recalling that each nonlinear partial differential equation requires individual treatment, we instead expand nonlinear terms in a series of Bessel functions (a Neumann series [24]). The use of a Neumann series instead of a Taylor expansion allows us to obtain expressions retaining intermode interactions even for the lowest order. This approach was previously used for the analysis of rotatory instability in a nonlinear interferometer with field rotation [25].

After obtaining a finite-order system of equations for the mode amplitudes we use the slaving principle [26]. This principle is realized here in the form of winner-takes-all (WTA) dynamics, now a popular model in the field of artificial neural networks [27,28] and in life in general.

This approach allows us to reduce the dimensionality of the unstable manifold and obtain elementary dynamic structures with minimum manifold dimension: the set of individual rolls (elementary modes) and hexagons. We consider hexagons as systems of interacting individual rolls with cooperative dynamics. Examples of interactions between these elementary dynamic structures are given, and we show that it is better for individual rolls to be involved in the competition as part of a hexagon.

This treatment goes beyond most WTA analyses in that we consider a spatially extended system having a continuous degeneracy of unstable Fourier modes caused by rotational symmetry in the transverse plane. Our analysis highlights the effects of input phase distortions, for which there is no obvious parallel in fluid systems. In particular, we demonstrate the importance of these effects in the making—and breaking—of hexagonal structures.

MATHEMATICAL MODEL

The system shown in Fig. 1(a) has been well discussed in the nonlinear optics literature. Correspondingly, we simply give the equations and refer to the relevant articles [2,4].

Kerr slice dynamics is described by a nonlinear diffusion equation for the nonlinear phase modulation $u(\vec{r},t)=lk\Delta n(\vec{r},t)$, where $k=2\pi/\lambda$, l is slice thickness and Δn is change in the refractive index due to the interaction of light with the slice:

$$\tau\frac{\partial u}{\partial t}+u=l_D^2\nabla_\perp^2 u+\Re|A(\vec{r},z=0)|^2+\Re|A(\vec{r},z=L,t)|^2 . \tag{1}$$

Here $\nabla_\perp^2$ is the Laplacian in the x and y directions describing transverse diffusion in the nonlinear medium with diffusion length l_D, τ is response time of the nonlinearity, and $\Re$ is the nonlinearity parameter.

The driving terms on the extreme right of (1) represent the effects of the direct and feedback intensities. The total distance from Kerr slice to mirror and back is equal to L. We consciously ignore several interesting effects connected with the feedback time delay and assume that $\tau\gg L/c$. Moreover, instead of a real laser beam of definite width, we study the somewhat unusual case of an input light field with uniform amplitude and nonuniform phase $\varphi(\vec{r})$. In this intermediate case the input field is no longer a plane wave, but in some sense still approximates the behavior of a plane wave:

$$A(\vec{r},z=0)=A_{\text{in}}=A_0\exp[i\varphi(\vec{r})] . \tag{2}$$

Finally, the complex amplitude of the optical field after traveling a distance z beyond the slice is defined as $A_0\cdot A(\vec{r},z,t)$, i.e., we normalize it to the input amplitude A_0, which is then incorporated into the nonlinearity parameter $\Re$.

These manipulations of the input field allow us to omit the term $\Re|A(\vec{r},z=0)|^2=\Re A_0^2$ in Eq. (1), as its presence can cause only an unimportant spatially homogeneous phase shift. A second advantage in form (2) is that the mathematical models coincide for both optical schemes under discussion [Figs. 1(a) and 1(b)] [23].

The normalized Eq. (1), free of insignificant terms and constants, becomes

$$\tau\frac{\partial u}{\partial t}+u=D\nabla_\perp^2 u+K|A(\vec{r},L,t)|^2 , \tag{3}$$

where D is a normalized diffusion coefficient and $K=\Re A_0^2$ is one of three key parameters of the problem: K, D, L. All parameters on which the nonlinear interaction depends are contained in K: A_0^2, n_2, k, l, R, where n_2 is nonlinear refractive index and R is the feedback mirror reflection coefficient. We can consider K as a control or bifurcation parameter. Our definition for u implies that K has the same sign as n_2, viz., $K>0$ for a self-focusing medium, and $K<0$ for a self-defocusing medium. We assume that K is switched on at $t=0$ from below the instability threshold, where u is very small, to a value for which some spatial frequencies begin to grow. We examine the growth and interaction of these components, with K assumed constant for $t>0$.

To complete the mathematical description requires the free-space propagation equation

$$-2i\frac{\partial A}{\partial z}=\nabla_\perp^2 A , \tag{4}$$

with boundary condition determined outside the Kerr slice

$$A(\vec{r},0,t)=\exp[iu(\vec{r},t)+i\varphi(\vec{r})] . \tag{5}$$

In (4) we normalized $\vec{r}$ by a and z by z_d (a and $z_d=ka^2$ are the aperture size of the Kerr slice and the diffraction length).

Note that the question of the normalization of spatial variables in (1)–(4) is rather delicate. For a laser beam of definite width the diameter a is a natural spatial scale

of the problem and the distance z can be normalized by z_d. In our case of unlimited aperture, diffractive effects are determined by the spatial scale of induced phase distortions in the Kerr slice. The minimum spatial size of these distortions can be restricted by diffusion with the characteristic length l_D. Certainly we could scale z to $l_D^2 k$. However, using this normalization we cannot make the transition to the case of $l_D=0$. There is a further restriction of the minimum spatial scale and thus again the size a of the input beam in the Kerr slice. For phase distortions with a spatial scale a_φ the diffraction-limited spot diameter at the distance L is $a_s=L/(ka_\varphi)$. For these distortions feedback can be regarded as closed only if $a_s \le a$, that is, $a_\varphi > a_\varphi^{\min}=L/(ka)$. It means that for a more correct statement of the problem we need to take into account the aperture diameter a. Nevertheless we need to do this only for the reflected field in the plane of the Kerr slice in order to cut off high spatial frequencies.

EQUATIONS FOR MODE AMPLITUDES

Consider a solution of (3) as a series of a large number N of discrete spectral components:

$$u(\vec{r},t)=\sum_{n=1}^{N} b_n^s \sin(\psi_n)+\sum_{n=1}^{N} b_n^c \cos(\psi_n) , \tag{6}$$

where $\psi_n=\vec{k}_n\cdot\vec{r}$ and $b_n^s(t), b_n^c(t)$ are real mode amplitudes, and $\vec{k}_n$ represents the wave vectors. The "distance" $|\vec{k}_n-\vec{k}_m|$ between the separate wave vectors $\vec{k}_n$ and $\vec{k}_m$ can be very small but nevertheless we have a discrete spectrum and separate modes. Represent (6) in the following form:

$$u(\vec{r},t)=\sum_{n=1}^{2N} b_n \sin(\psi_n) , \tag{7}$$

where

$$b_n=\begin{cases} b_n^s, & n=1,\ldots,N \\ b_n^c, & n=N+1,\ldots,2N , \end{cases}$$

and

$$\psi_n=\begin{cases} \vec{k}_n\cdot\vec{r}, & n=1,\ldots,N \\ \vec{k}_n\cdot\vec{r}+\pi/2, & n=N+1,\ldots,2N . \end{cases}$$

We must choose the same type of series to describe both the initial condition and phase distortion function φ:

$$u(\vec{r},0)=\sum_{n=1}^{2N} b_n^0 \sin(\psi_n) , \tag{8}$$

$$\varphi(\vec{r})=\sum_{n=1}^{2N} \varphi_n \sin(\psi_n) . \tag{9}$$

Many, or indeed all, of the φ_n may be zero, the latter case describing an ideal plane wave input.

Substituting (7) into (5) yields the expression for complex amplitude A just beyond the Kerr slice:

$$A(\vec{r},0,t)=\prod_{n=1}^{2N} \exp[ia_n(t)\sin(\psi_n)] , \tag{10}$$

where $a_n=b_n+\varphi_n$.

The physical sense of this expression is clear. Each term in (10) describes a plane wave passed through a harmonic phase grating with depth of modulation a_n and spatial frequency $\vec{k}_n$.

Using the standard expansion of the exponential terms in (10) gives

$$A(\vec{r},0,t)=\prod_{n=1}^{2N}\left[J_0(a_n)+2i\sum_{j=1}^{\infty} J_{2j-1}(a_n)\sin[(2j-1)\psi_n]+2\sum_{j=1}^{\infty} J_{2j}(a_n)\cos(2j\psi_n)\right] . \tag{11}$$

We assume that mode amplitudes in the vicinity of the bifurcation point are small enough for us to keep in the Neumann expansion (11) only the terms up to second order in J_1, first order in J_2, and to neglect all J_n for $n \ge 3$. Then

$$A(\vec{r},0,t)\simeq\left[\prod_{n=1}^{2N} J_0(a_n)\right]\left[1+2i\sum_{n=1}^{2N} Q_n\sin(\psi_n)+2\sum_{n=1}^{2N} P_n\cos(2\psi_n)+2\sum_{n=1}^{2N}\sum_{m=1}^{n-1} Q_m Q_n[\cos(\psi_n+\psi_m)-\cos(\psi_n-\psi_m)]\right] , \tag{12}$$

where $Q_n=J_1(a_n)/J_0(a_n)$ and $P_n=J_2(a_n)/J_0(a_n)$ are normalized Bessel functions. This truncation shows that the set (6) of wave vectors and phases must include all second harmonics, sums, and differences of $\vec{k}_n$ to obtain closure. One way to achieve this is to assume that $\vec{k}_n$ constitutes an infinite space-periodic lattice. By making the unit cell small enough, the wave vector continuum can be approximated as closely as desired. Such a discretization remains valid after we form the intensity $|A|^2$, and indeed for the full Neumann series. Notice that in accordance with (12) the complex amplitude $A(\vec{r},0,t)$ is the sum of plane waves with different wave vectors $\vec{k}_n$.

The solution of the free-space propagation equation at a distance z can be easily obtained by multiplying each plane-wave component by the propagation term $\exp(-ik_n^2 z)$ [29]. The feedback field in the Kerr slice is then given by

$$A(\vec{r},L,t)\simeq 2D_0\left\{1/2+i\sum_{n=1}^{2N}Q_n\exp(-ik_n^2L)\sin(\psi_n)+\sum_{n=1}^{2N_1}P_n\exp(-4ik_n^2L)\cos(2\psi_n)\right.$$
$$+\sum_{n=1}^{2N_2}\sum_{m=1}^{n-1}Q_mQ_n\exp(-i|\vec{k}_n+\vec{k}_m|^2L)\cos(\psi_n+\psi_m)$$
$$\left.-\sum_{n=1}^{2N_2}\sum_{m=1}^{n-1}Q_mQ_n\exp(-i|\vec{k}_n-\vec{k}_m|^2L)\cos(\psi_n-\psi_m)\right\}, \tag{13}$$

where $D_0=\prod_{n=1}^{2N}J_0(a_n)$. In (13) we take advantage of the finite Kerr slice diameter. The Kerr slice aperture truncates high spatial frequency components. As a result the numbers N_1 and N_2 appear in (13). Thus the first reduction in manifold dimension occurs due to the finite aperture. Instead of calculating N_1 and N_2 we take into account the spatial frequency threshold $k_{\max}=(a_\varphi^{\min}/a)^{-1}=1/L$ where the distance L is normalized by z_d. In the following development we assume that all important wave vectors are less than $k_{\max}$ and thus write the corresponding series without the upper indices.

In the same second-order Neumann approximation we obtain the following expression for normalized feedback intensity:

$$I(\vec{r},L,t)=|A(\vec{r},L,t)|^2\simeq 4(D_0)^2\left\{1/4+(1/2)\sum_n Q_n^2+\sum_n Q_n\sin(k_n^2L)\sin(\psi_n)+\sum_n[P_n\cos(4k_n^2L)-(1/2)Q_n^2]\cos(2\psi_n)\right.$$
$$-\sum_n\sum_{m=1}^{n-1}Q_nQ_m\{\cos(|\vec{k}_n-\vec{k}_m|^2L)-\cos[(k_n^2-k_m^2)L]\}\cos(\psi_n-\psi_m)$$
$$\left.+\sum_n\sum_{m=1}^{n-1}Q_mQ_n\{\cos(|\vec{k}_n+\vec{k}_m|^2L)-\cos[(k_n^2-k_m^2)L]\}\cos(\psi_n+\psi_m)\right\}. \tag{14}$$

Substituting (6) and (14) into Eq. (3) for the nonlinear phase modulation gives

$$\sum_n[\tau\dot{a}_n+(1+Dk_n^2)(a_n-\varphi_n)]\sin\psi_n=KI(\vec{r},L,t)\ . \tag{15}$$

Consider the simplest case when the initial mode amplitudes $a_n^0=a_n(0)$ belong to a $2N$-dimensional sphere in the space of mode amplitudes, with a small radius $\epsilon_0\ll 1$. Select a second sphere with radius $\epsilon_1>\epsilon_0$. Inside this second sphere the amplitudes a_n are small enough to keep in (14) terms up to the first order of the Bessel functions. The original system dynamics are analyzed only up to time t_1, at which the system trajectory crosses the surface of sphere ϵ_1. As an estimate let $J_2(\epsilon_1)=0.1J_1(\epsilon_1)$, which yields $\epsilon_1\simeq 0.4$ (not such a small sphere).

Inside sphere ϵ_1 (15) reduces to

$$\tau\dot{a}_n+(1+Dk_n^2)(a_n-\varphi_n)=4K\sin(k_n^2L)\left[\prod_{j=1}^{2N}J_0^2(a_j)\right]Q_n\ ,$$
$$n=1,\ldots,2N\ . \tag{16}$$

Note that although we have used in (15) only the first-order Neumann approximation we have kept intermode interactions. The collective term $D_0^2=\prod_{j=1}^{2N}J_0^2(a_j)$ describes the influence of the system state on individual mode behavior.

LINEAR STABILITY ANALYSIS; INFLUENCE OF PHASE DISTORTIONS

In the tradition of nonlinear dynamics we start from a linear stability analysis. In the first order of a Taylor expansion [$J_0(a_n)\simeq 1$, $J_1(a_n)\simeq a_n/2$], instead of (16) we obtain, using a modified notation and generalizing to allow for input phase distortions, the known system of equations [2]

$$\tau\dot{a}_n+(1+Dk_n^2)(1-K/K_{\text{th}}^n)a_n=(1+Dk_n^2)\varphi_n\ , \tag{17}$$

where

$$K_{\text{th}}^n=(1+Dk_n^2)/[2\sin(k_n^2L)]\ . \tag{18}$$

There are no intermode interactions in this case, meaning feedback occurs separately for each individual mode. Neglecting phase distortions we obtain the excitation condition for the nth mode

$$K/K_{\text{th}}^n>1\ , \tag{19}$$

and the eigenvalues λ_n for the nonlinear system of equations (16) in the neighborhood of the stationary point $a_n=0$:

$$\lambda_n=-(1+Dk_n^2)(1-K/K_{\text{th}}^n)\ . \tag{20}$$

If (19) holds the corresponding eigenvalue is positive. The sine function in (18) arising from propagation must have the same sign as the nonlinearity K for this to occur. In Fig. 2 the threshold curves for a self-defocusing medium ($K<0$) are shown. Notice the gap at small wave vectors. A self-focusing medium would show instabilities in this and subsequent gaps. By changing the aperture size a or the threshold spatial frequency $k_{\max}$ it is possible to control the number of instability branches. We ignore the influence of the aperture a for calculation of the outgoing wave amplitude $A(\vec{r},L,t)$. A more complete

analysis of the problem for a beam with Gaussian intensity distribution gives [30]

$$K_{\text{th}}^{n}=(1+Dk_n^2)/[2g_n\sin(k_n^2L)]\ , \tag{21}$$

where $g_n=g(k_nL)$ are values of the Gaussian aperture function $g(\vec{r})=\exp(-r^2)$ at the points k_nL (assume $k_nL\gg 1$). Expression (21) indicates that the minimum threshold in each branch increases with wave vector. This means the lowest branch will usually dominate the dynamics.

We omit the rigorous algebraic manipulations that lead to expression (21). The physical meaning behind the weighting coefficients g_n is rather obvious. After traveling a distance L the plane-wave component having wave vector $\vec{k}_n$ obtains the linear "shift" $\Delta=\sin(\alpha_n)\hat{L}=(\hat{k}_m/k)\hat{L}$, where $k=2\pi/\lambda$ (all parameters now have dimensions). The intensity of the "shifted" portion of this plane wave in the plane of the Kerr slice is determined by $g(\Delta/a)$. Taking into account the expression for Δ and normalizations introduced earlier, we obtain a factor that decreases the feedback intensity coefficient $g_n=g(k_nL)$.

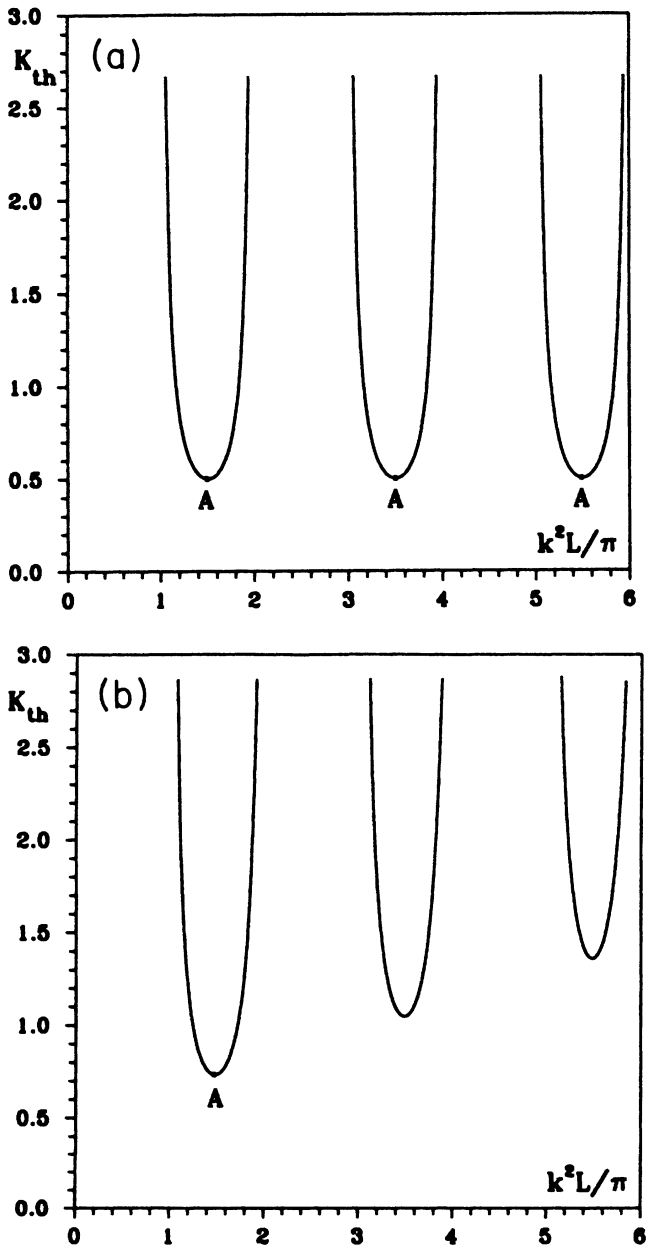

FIG. 2. Threshold curves for a self-defocusing Kerr slide. (a) $L=0.1$, $D=0$, $k_{\max}^2L/\pi=12.7$ (due to aperture effects there are six active branches); (b) $L=0.1$, $D=0.01$.

Now consider in the linear approximation the influence of phase distortions. The stationary-state amplitudes $\hat{a}_n$ are determined by

$$\hat{a}_n=\varphi_n/(1-K/K_{\text{th}}^{n})\ . \tag{22}$$

In stable regions where $(1-K/K_{\text{th}}^{n})>1$, input phase distortions are suppressed ($|\hat{a}_n|<|\varphi_n|$). But in the vicinity of bifurcation, phase distortions are amplified. Note, that (22) is reasonable only for quite small phase perturbations (when $|\varphi_n|\ll 1$).

ACTIVE MODES AND THE FIRST MANIFOLD DIMENSION REDUCTION

Consider the nonlinear system (16) for mode amplitudes, which can be related to the well-known order-parameter equations [26]. There is no general method for an analysis of these systems, but there is a common tendency: to reduce the manifold dimension. In the vicinity of the bifurcation point this reduction can be justified on the basis of a slaving principle [26].

According to this principle, in the vicinity of a critical point the solution of the original system (16) asymptotically approaches the solution of a system with lower manifold dimension. The reduced system includes only $2M$ equations corresponding to the modes having nonnegative eigenvalues $\lambda_m\geq 0$, $m=1,\ldots,2M$ (the *active* modes):

$$\tau\dot{a}_m+(1+Dk_m^2)(a_m-\varphi_m)$$
$$=4K\sin(k_m^2L)\left[\prod_{j=1}^{2M}J_0^2(a_j)\right]J_1(a_m)/J_0(a_m)\ ,$$
$$m=1,\ldots,2M<2N\ . \tag{23}$$

We enumerate these equations in order of decreasing eigenvalues:

$$\lambda_1\geq\lambda_2\geq\cdots\geq\lambda_{2M}\geq 0\ .$$

In the linear approximation, equations for amplitudes a_n^s and a_n^c coincide and $\lambda_l=\lambda_{l+M}$, $l=1,\ldots,M$. The remaining $2(N-M)$ modes either die or survive only because they are driven by the active modes (or the phase distortions). In either case their amplitudes remain small, and hardly affect those of the active modes.

Note that we can apply the slaving principle only for a special type of initial condition: the initial a_m^0 of the active modes (AM) are inside the small sphere ϵ_0 centered on the stationary point with all $a_m=0$. This reduction means we can ignore the influence of modes with negative eigenvalues (the passive modes).

WTA—DYNAMICS AND THE SECOND REDUCTION OF THE MANIFOLD DIMENSION

Assuming that K is not too far above threshold, active modes (with $\lambda_m > 0$) lie on one or more annuli in the transverse k space. On the combined basis of analytical and numerical evidence it appears that the first effects of nonlinear coupling arise as competition among active modes, rapidly shrinking these annuli down to a set of "superactive modes" (SAM) lying on or very near the k-space circle of modes with maximal eigenvalue (points A on the threshold curves shown in Fig. 2). Exceptionally, in the presence of degeneracy several circles of SAM may exist. The SAM are still very numerous—in the continuum limit there are an infinite number. We demonstrate below the presence of winner-take-all dynamics in this system, which acts to kill off all but one, or a few SAM. WTA dynamics has been little studied for spatially extended systems such as the present one [17,25].

Consider the problem of intermode interactions in our first-order Neumann-series approximation. The reduced system of equations (23) can be related to systems of artificial neural networks [31]. Thus we rewrite (23) in a form similar to neural network models:

$$\tau \dot{a}_m / a_m = -(1+Dk_m^2) + f_m(a_1, \ldots, a_{2M}) , \tag{24}$$

where we have temporarily neglected phase distortions, and where

$$f_m = 2(1+Dk_m^2)(K/K_{\text{th}}^m) \left[\prod_{j=1}^{2M} J_0^2(a_j) \right] \times [J_1(a_m)/a_m]/J_0(a_m) , \tag{25}$$

with $m = 1, \ldots, 2M$. Note that f_m is an even function of a_m, i.e., a function of the "intensities" of the modes only.

In the case where

$$\frac{\partial f_m}{\partial a_j} \le 0 \tag{26}$$

for all $j \neq m$ in the system of equations in (24), the WTA condition of competition is fulfilled. The condition given in (26) states that an increase in the intensity of any of the active modes (for example, a_j) decreases the growth rate for the remaining amplitudes. Any mode whose growth rate is driven negative begins to decay, and in doing so enhances the growth rates of all the others, again through (26). The winner of this competition will be that one mode whose initial growth rate and amplitude best fit it for the struggle. That our system possesses such WTA dynamics can be seen by inspection. The coupling function f_m is a product of positive definite terms, at least while all amplitudes remain small enough that no Bessel function changes sign. Since J_0 is a decreasing function in this range, the WTA condition is satisfied.

Figure 3 gives some examples of the WTA behavior exhibited by (23) for a small body of active modes. These modes were in two groups of six modes. The modes within each group has the same value for the threshold parameter: $K_{\text{th}}^m = K_{\text{th}}^{(1)}$ for the first six modes and $K_{\text{th}}^m = K_{\text{th}}^{(2)}$ ($K_{\text{th}}^{(1)} \le K_{\text{th}}^{(2)}$) for the second group.

On what does the victory in the competition depend? Two factors are very important in the mode battle: the initial condition a_m^0 and the eigenvalues λ_m, or equivalently, the parameters

$$D^{(m)} = (K - K_{\text{th}}^m)/K_{\text{th}}^m = \lambda_m/(1+Dk_m^2) , \tag{27}$$

which are more convenient for us. If growth rates were constant then a mode whose growth rate exceeded that of another by $\Delta\lambda$ but with initial amplitude smaller by a factor C, would nonetheless overtake it in a time of order $\log|C|/\Delta\lambda$. Thus if the initial sphere is small enough only the mode or modes with largest eigenvalue will survive. The effect of WTA competition in altering growth rates and the fact that (26) is valid only while all amplitudes remain small means the competition outcome is somewhat uncertain. We must therefore allow for the possibility that several, or even multiple, modes may survive until the time we must consider higher-order mode couplings.

Various aspects of intermode competition are shown in Fig. 3 for different parameters $D^{(1)}$ and $D^{(2)}$. Even a disadvantage in the initial conditions [Fig. 3(a)] did not spoil victory for the mode with the largest parameter $D^{(m)}$. More strenuous competition takes place between modes with similar values for the parameter $D^{(m)}$ [Fig. 3(b)]. Nevertheless, the result can be predicted because $D^{(1)} > D^{(2)}$. Result of the competition between the modes with equal parameters $D^{(m)}$ depends only on the initial condition [Fig. 3(c)]. As mentioned, modes a_m^s and a_m^c have equal wave vectors $\vec{k}_m$ and eigenvalues λ_m so that WTA competition determines the phase of the rolls that have the advantage in growth rate. Note that the competition's decisive events take place inside sphere ϵ_1 where expression (23) is valid.

Using this analysis allows a second reduction in manifold dimension so that we keep only a small body of potential winner modes located at the bottom of the instability branches (the points A in Fig. 2). We also keep a few modes that have an advantage in initial conditions and only slightly lower values for the $D^{(m)}$ parameters.

Even in the case of a large degeneracy for the largest eigenvalue λ_1 (e.g., on a circle in k space) WTA competition between these modes still ensures that only a small number of modes (differentiated by the azimuth angle on the circle) survive. At this stage, which angle survives depends only on initial conditions.

In the presence of small phase distortions this picture of intermode competition changes somewhat (Fig. 4). As in the previous case, the advantage lies with the mode having the largest value for the parameter $D^{(m)}$ [Fig. 4(a)]. Among equivalent modes the victory will go to the mode with the maximum phase distortion coefficient [Fig. 4(b)]. With increasing phase distortion WTA dynamics is destroyed [Fig. 4(c)].

SECOND-ORDER EQUATIONS FOR SUPERACTIVE MODES AND HEXAGON APPEARANCE

What happens to superactive modes that survive the competition inside sphere ϵ_1 to reach the moment t_1

when one mode amplitude crosses the boundary of this sphere? Define a larger sphere with radius $\epsilon_2 > \epsilon_1$ that is still small enough to ensure that the second-order Bessel function approximation in (14) and (15) is valid. For an estimate, $J_3(\epsilon_2)=0.1J_2(\epsilon_2)$ gives $\epsilon_2 \simeq 0.65$.

We need to separate the spatial and time-dependent functions in (15) and to obtain a closed system of equations for the SAM amplitudes. In accordance with our scenario of the intermode competition, inside sphere ϵ_2 we need to take into account the second-order Bessel function terms in (14) only for the SAM amplitudes, with wave-vectors located at the bottom of the instability branches (points A in Fig. 2). Call these vectors $\vec{\kappa}_m$.

Assume that diffusion is strong enough or the Kerr slice aperture a is small enough to keep only the SAM amplitudes from the most unstable branch [the point A Fig. 2(b)], that is,

$$|\vec{\kappa}_m| = \kappa, \quad \mathrm{sgn}(K)\sin(\kappa^2 L) > 0, \quad m = 1, \ldots, M_s \, . \tag{28}$$

where M_s is the number of SAM wave vectors close to the bottom of this branch. From (14) the intensity is given by

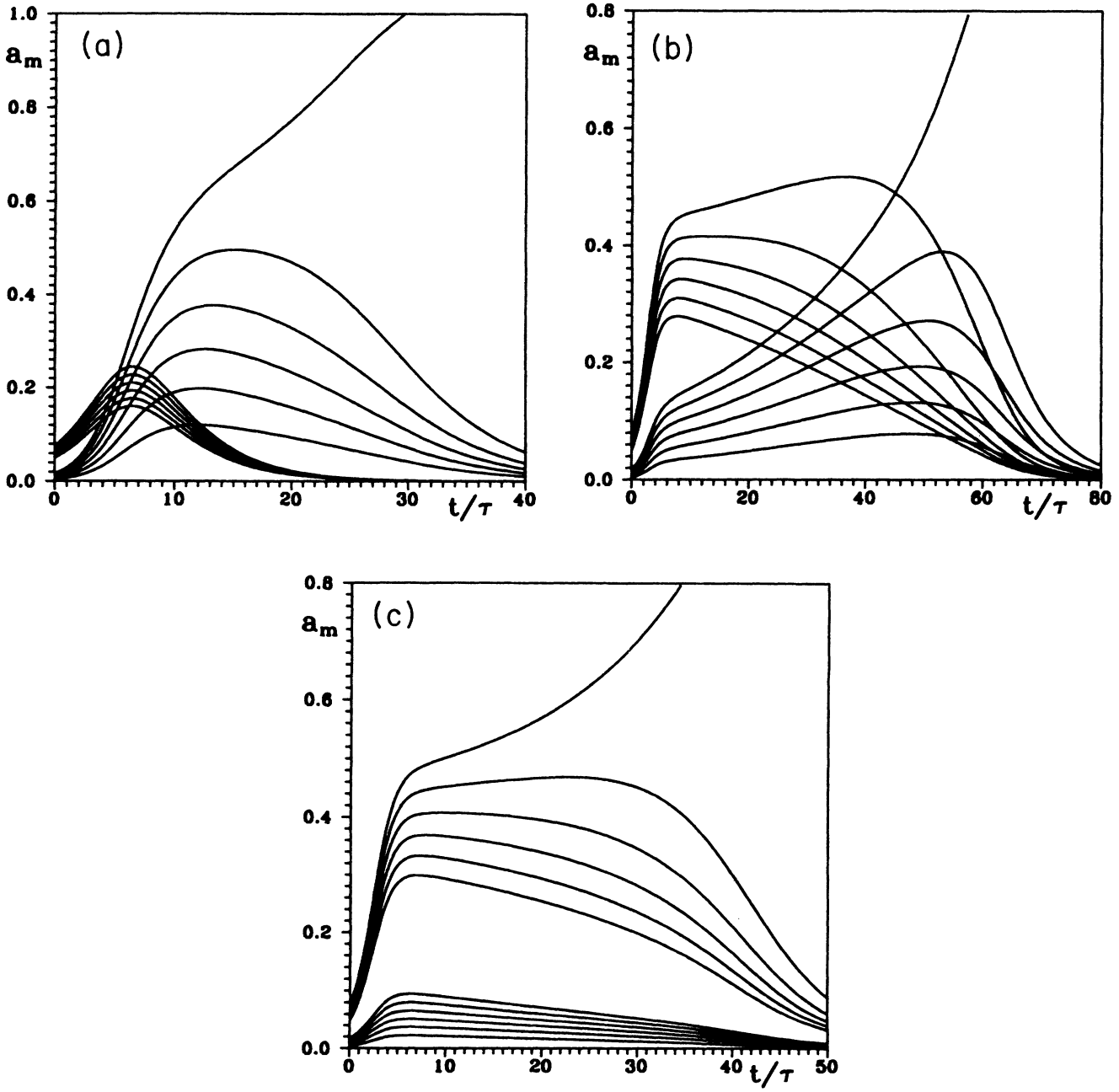

FIG. 3. WTA-type dynamics for active modes. Behavior of the solution to Eqs. (23) for $K=0.8$, $D=0$, $L=0.1$, $\varphi=0$, $a_m^0 < a_{m+1}^0$, $m=1,\ldots,11$. Parameters for the first group of modes ($m=1,\ldots,6$) are $k_m^{(1)}=6.86$, $K_{\mathrm{th}}^{(1)}=0.5$, $D^{(1)}=0.6$. Parameters for the second group of modes ($m=7,\ldots,12$) are (a) $k_m^{(2)}=7.31$, $K_{\mathrm{th}}^{(2)}=0.62$, $D^{(2)}=0.29$; (b) $k_m^{(2)}=7.09$, $K_{\mathrm{th}}^{(2)}=0.52$, $D^{(2)}=0.54$; (c) $k_m^{(2)}=6.86$, $K_{\mathrm{th}}^{(2)}=0.50$, $D^{(2)}=0.6$.

$$I(\vec{r},L,t)\simeq 4D_0^2[I^{(0)}+I^{(1)}+I^{(2)}+I^{(+)}+I^{(-)}] , \tag{29}$$

where

$$D_0=\prod_{n=1}^{2N} J_0(a_n) ,$$

$$I^{(0)}=1/4+(1/2)\sum_{n=1}^{2N} Q_n^2 ,$$

$$I^{(1)}=\sum_{m=1}^{2M_1} Q_m \sin(k_m^2 L)\sin(\psi_m) + \sin(\kappa^2 L)\sum_{m=1}^{2M_s} Q_m \sin(\psi_m) ,$$

$$I^{(2)}=\sum_{m=1}^{2M_s} [P_m \cos(4\kappa^2 L)-(1/2)Q_m^2]\cos(2\psi_m) ,$$

$$I^{(+)}=-\sum_{m=1}^{2M_s}\sum_{n=1}^{m-1} Q_m Q_n [1-\cos(|\vec{\kappa}_n+\vec{\kappa}_m|^2 L)] \times\cos(\psi_n+\psi_m) ,$$

$$I^{(-)}=\sum_{m=1}^{2M_s}\sum_{n=1}^{m-1} Q_m Q_n [1-\cos(|\vec{\kappa}_n-\vec{\kappa}_m|^2 L)] \times\cos(\psi_n-\psi_m) .$$

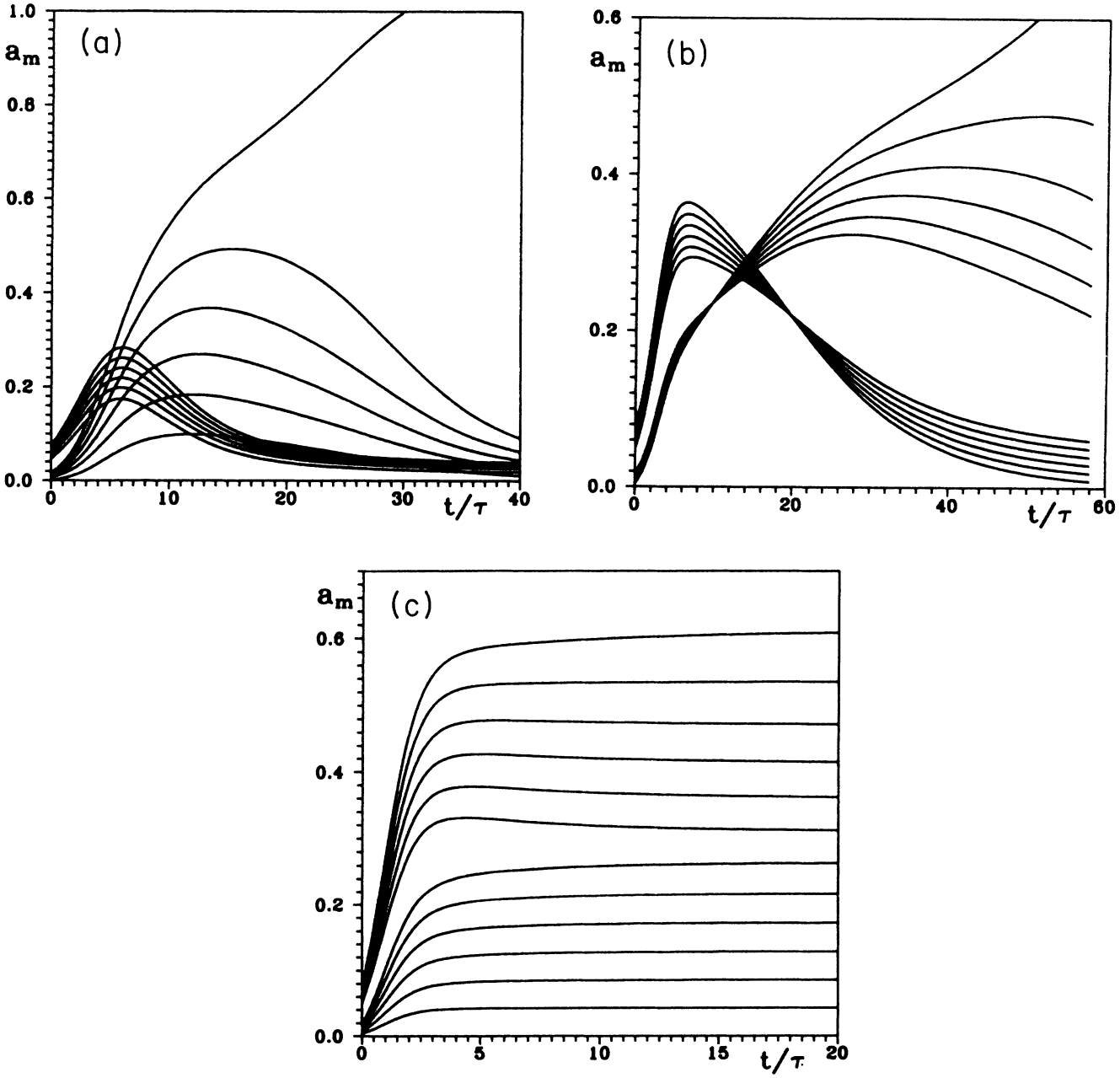

FIG. 4. Intermode competition in the presence of phase distortions: (a) $\varphi_m=0.001m$, $m=1,\ldots,12$ [all parameters correspond to Fig. 3(a)]; (b) $\varphi_m=0.001(12-m)$, $m=1,\ldots,12$ [all parameters correspond to Fig. 3(b)]; (c) $\varphi_m=0.01m$, $m=1,\ldots,12$ [all parameters correspond to Fig. 3(c)].

In (29) $N=M_1+M_s$, where M_1 is the number of active mode wave vectors inside sphere ϵ_1 that have not died as of the moment t_1. The $I^{(2)}$ term has wave vector $2\vec{\kappa}_m$, which in general is that of a passive mode and is insignificant except at large amplitudes. The same is true for terms bilinear in the Q's unless $\vec{\kappa}_m+\vec{\kappa}_n=\vec{\kappa}$ or $\vec{\kappa}_m-\vec{\kappa}_n=\vec{\kappa}$, which occurs when $\vec{\kappa}_m$ and $\vec{\kappa}_n$ make an angle of $\pi/3$ or $2\pi/3$ (Fig. 5). These terms are associated with hexagon formation.

We cannot yet equate components in (15) with equivalent wave-vector values because they contain different phase shifts $\psi_m+\psi_n$ and $\psi_m-\psi_n$. In the first-order Neumann approximation (inside sphere ϵ_1) the behavior of mode $a_n(t)\sin\psi_n$ depends only on the amplitude a_n. Outside sphere ϵ_1 we must account for the relationship between amplitudes a_l^s and a_l^c (the sine and cosine components) that determine the time-dependent phase $\mu_l(t)$ of the original mode with the wave vector $\vec{\kappa}_l[\tan(\mu_l)=a_l^c/a_l^s]$.

Now examine the couple of superactive modes with wave vector $\vec{\kappa}_l$

$$\Phi_l=a_l^s(t)\sin(\vec{\kappa}_l\cdot\vec{r})+a_l^c(t)\cos(\vec{\kappa}_l\cdot\vec{r}) ,$$
$$l=1,\ldots,M_s , \quad (30)$$

to find the components of feedback intensity that affect the behavior of these modes. First separate all the components in (29) having wave vector $\vec{\kappa}_l$. The vector $\vec{\kappa}_l$ can be obtained as a result of the superposition of different wave vectors. For completeness we amend our definition of SAM so as to require that M_s include all five "partners" of any $\vec{\kappa}_l$ contributing to a hexagon at that $\vec{\kappa}_l$. We further assume that no other pairs combine to give a wave vector lying on the SAM circle. This is always true for a sufficiently coarse discretization of the k plane, or, more generally, to the WTA competition, thus leaving only isolated survivors on that circle.

Figure 5 shows a group of six vectors $\vec{\kappa}_{m,l}$, $(l=0,\ldots,5)$ forming a regular hexagon (the hexagon "family"). Define $m=1,\ldots,M_f$ to be a hexagon group index with M_f the number of mode families. Then the terms $I^{(+)}$ and $I^{(-)}$ in (29) can be written in the following form:

$$I^{(+)}=\sum_{m=1}^{M_f}\sum_{l=0}^{5} I_{m,l}^{(+)}, \quad I^{(-)}=\sum_{m=1}^{M_f}\sum_{l=0}^{5} I_{m,l}^{(-)} , \quad (31)$$

where

$$I_{m,l}^{(+)}=C_m(Q^c_{m,[l+1]}Q^c_{m,[l+5]}-Q^s_{m,[l+1]}Q^s_{m,[l+5]})\cos(\vec{\kappa}_{m,l}\cdot\vec{r})+C_m(Q^c_{m,[l+1]}Q^s_{m,[l+5]}+Q^s_{m,[l+1]}Q^c_{m,[l+5]})\sin(\vec{\kappa}_{m,l}\cdot\vec{r}) ,$$

$$I_{m,l}^{(-)}=C_m[(Q^c_{m,[l+1]}Q^c_{m,[l+2]}+Q^s_{m,[l+1]}Q^s_{m,[l+2]})+(Q^c_{m,[l+5]}Q^c_{m,[l+4]}+Q^s_{m,[l+5]}Q^s_{m,[l+4]})]\cos(\vec{\kappa}_{m,l}\cdot\vec{r})$$
$$+C_m[(Q^s_{m,[l+1]}Q^c_{m,[l+2]}-Q^c_{m,[l+1]}Q^s_{m,[l+2]})+(Q^s_{m,[l+5]}Q^c_{m,[l+4]}-Q^c_{m,[l+5]}Q^s_{m,[l+4]})]\sin(\vec{\kappa}_{m,l}\cdot\vec{r}) , \quad (32)$$

and $Q^s_{m,l}=J_1(a^s_{m,l})/J_0(a^s_{m,l})$, $Q^c_{m,l}=J_1(a^c_{m,l})/J_0(a^c_{m,l})$, and $a^s_{m,l}$, $a^c_{m,l}$ are mode amplitudes of the hexagon family; also, define in (32) that $[l]=(l\bmod 6)$ and $C_m=[1-\cos(\kappa_m^2 L)]$.

Previously we asserted that the WTA-type system (24) correctly describes early evolution and competition. It appears that if we use a Taylor rather than a Neumann expansion $I^{(+)}$ or $I^{(-)}$, which is second order in the amplitudes, it should be considered prior to the occurrence of competing terms in (24) which are of third order. This is not so. In the early stages when there are many active modes any one mode will have numerous source terms arising from $I^{(+)}$ and $I^{(-)}$. These contribute with random phases, and will normally be insignificant in comparison with the phase-independent third-order couplings through the J_0 terms in (23) and (24). Thus the Neumann series correctly orders the significant terms in the early evolution.

Substituting the cosine and sine components into (15) we obtain equations for the hexagon family's SAM amplitudes inside the second sphere:

$$\tau\dot{a}^s_{m,l}+(1+D\kappa_m^2)\cdot(a^s_{m,l}-\varphi^s_{m,l})=F^s_{m,l} ,$$
$$\tau\dot{a}^c_{m,l}+(1+D\kappa_m^2)\cdot(a^c_{m,l}-\varphi^c_{m,l})=F^c_{m,l} , \quad (33)$$

where

$$F^s_{m,l}=4K(D_0^f)^2(D_0)^2\{S_m Q^s_{m,l}+C_m[(Q^s_{m,[l+1]}Q^c_{m,[l+5]}+Q^c_{m,[l+1]}Q^s_{m,[l+5]})+(Q^s_{m,[l+1]}Q^c_{m,[l+2]}-Q^c_{m,[l+1]}Q^s_{m,[l+2]})$$
$$+(Q^s_{m,[l+5]}Q^c_{m,[l+4]}-Q^c_{m,[l+5]}Q^s_{m,[l+4]})]\} , \quad (34)$$

and

$$F^c_{m,l}=4K(D_0^f)^2(D_0)^2\{S_m Q^c_{m,l}+C_m[(Q^c_{m,[l+1]}Q^c_{m,[l+5]}-Q^s_{m,[l+1]}Q^s_{m,[l+5]})+(Q^c_{m,[l+1]}Q^c_{m,[l+2]}+Q^s_{m,[l+1]}Q^s_{m,[l+2]})$$
$$+(Q^c_{m,[l+5]}Q^c_{m,[l+4]}+Q^s_{m,[l+5]}Q^s_{m,[l+4]})]\} . \quad (35)$$

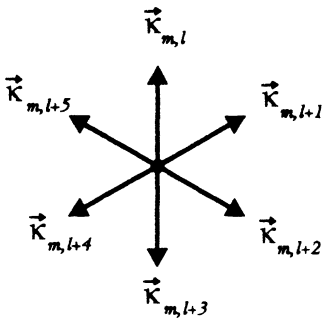

FIG. 5. A group of six wave vectors forming a hexagon. There are three different pairs of wave vectors contributing to $\vec{k}_l$.

Here $m=1,\ldots,M_f$; $l=0,\ldots,5$; $S_m=\sin(\kappa_m^2 L)$; and

$$D_0^f=\prod_{m=1}^{M_f}\prod_{j=0}^{5}[J_0(a^s_{m,j})J_0(a^c_{m,j})]\ ,$$

$$D_0=\prod_{j=6M_f+1}^{N}[J_0(a^s_j)J_0(a^c_j)]\ .$$

Note that Eqs. (33) are not independent, since mode amplitudes for the wave vectors $\vec{\kappa}_{m,l}$ and $-\vec{\kappa}_{m,l}$ are linked as follows: $a^c_{m,[l]}=a^c_{m,[l+3]}$ and $a^s_{m,[l]}=-a^s_{m,[l+3]}$.

In fact, we have only six independent equations. Nevertheless it is more convenient for us to deal with the original system of equations (33).

The number of modes taking part in the system dynamics inside sphere ϵ_2 is $N=M_1+6M_f$. For a complete system of equations we must include equations for the active modes inside sphere ϵ_1 that have not died as of t_1:

$$\tau\dot{a}^s_n+(1+Dk_n^2)(a^s_n-\varphi^s_n)=4K(D_0^f D_0)^2 C_n Q^s_n\ , \tag{36}$$

$$\tau\dot{a}^c_n+(1+Dk_n^2)(a^c_n-\varphi^c_n)=4K(D_0^f D_0)^2 C_n Q^c_n\ , \tag{37}$$

$$n=6M_f+1,\ldots,N\ .$$

PHYSICS OF ELEMENTARY INTERACTIONS AND COOPERATIVE DYNAMICS

Let us investigate the relationships between neighboring modes inside the second sphere. Consider the following "elementary" interactions (Fig. 6).

(i) SAM $\Longleftrightarrow$ SAM. Interaction between very near familiar neighbors; cosine and sine type SAM $a^c_{m,l}$ and a_m, l^s, $l=0,1,\ldots,5$.

(ii) SAM $\Longleftrightarrow$ AM. Interaction between SAM and the active modes a^c_n, a^s_n, $n=1,\ldots,M_1$, which have not died in the ϵ_0 sphere.

(iii) AM $\Longleftrightarrow$ AM. Interaction between active modes. Interaction between the active modes in (36) and (37) is determined by the term $(D_0^f D_0)^2$. This suggests the WTA competition that occurs here is the same as the WTA competition inside sphere ϵ_1 ("ϵ_1 sphere dynamics").

(iv) SAM $\Longleftrightarrow$ AM+SAM. The pattern repeats. In (33)–(37) the hexagon family equations share the same "WTA term" which combines the influence of the active modes, with the net result that we again obtain WTA competition.

Explaining elementary interactions inside sphere ϵ_1 is not as simple. Let us analyze the nature of interactions in the hexagon family of SA modes (the members of this Φ_m mode family are $a^s_{m,l}$ and $a^c_{m,l}$, $l=0,\ldots,5$). First calculate the partial derivatives:

$$\frac{\partial F^c_{m,l}}{\partial a^{s,c}_{m,[l+i]}},\quad \frac{\partial F^s_{m,l}}{\partial a^{s,c}_{m,[l+i]}}\ , \tag{38}$$

where the functions $F^s_{m,l}$, $F^c_{m,l}$ are determined by expressions (34) and (35).

Using the formulas for Bessel functions [24] we obtain for the first-order approximation:

$$\frac{\partial F^c_{m,l}}{\partial a^c_{m,[l+i]}}=TC_m\times\begin{cases}Q^c_{m,[l+5]}+Q^c_{m,[l+2]}, & i=1\\ Q^c_{m,[l+1]}, & i=1\\ 0, & i=3\\ Q^c_{m,[l+5]}, & i=4\\ Q^c_{m,[l+1]}+Q^c_{[l+4]}, & i=5\end{cases}+O_{c,c}(Q^{s,c}_m)\ , \tag{39}$$

$$\frac{\partial F^c_{m,l}}{\partial a^s_{m,[l+i]}}=TC_m\times\begin{cases}-Q^s_{m,[l+5]}+Q^s_{m,[l+2]}, & i=1\\ Q^s_{m,[l+1]}, & i=2\\ 0, & i=3\\ Q^s_{m,[l+5]}, & i=4\\ -Q^s_{m,[l+1]}+Q^s_{[l+4]}, & i=5\end{cases}+O_{c,s}(Q^{s,c}_m)\ , \tag{40}$$

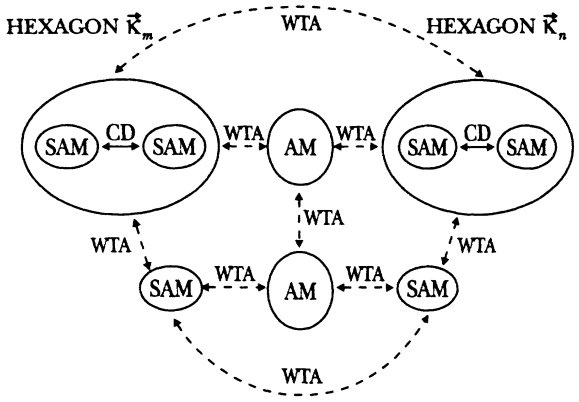

FIG. 6. Intermode interactions that occur during the pattern formation process. "WTA" represents "winner-takes-all" dynamics (dashed arrows); "CD" represents cooperative dynamics (continuous arrows).

where $T=4K(D_0^f D_0)^2$ and $O_{c,c}(Q_m^{c,s})$, $O_{c,s}(Q_m^{s,c})$ are second-order terms. Similar formulas are possible for $\partial F_{m,l}^s/\partial a_{m,[l+i]}^{s,c}$ as well.

The complicated brackets in (39) and (40) demonstrate the unequal rights in the mode family, but here another circumstance is more important. Taking into account second-order terms in mode equation (33) (i.e., transition to sphere ϵ_2) we obtain the first-order response for intermode terms in (39) and (40). So it is dangerous to omit second-order terms when trying to analyze intermode interactions.

Let us analyze a special type of solutions $a_{m,l}^s=0$, $a_{m,l}^c\neq 0$ of Eq. (33). Then for $a_{m,l}^c(0)>0$, $K>0$ or $a_{m,l}^c(0)<0$, $K<0$ inside spheres ϵ_1 and ϵ_2 for all partial derivatives in (39), we obtain

$$\frac{\partial F_{m,l}^c}{\partial a_{m,[l+i]}^c}>0 \ . \tag{41}$$

In this case within the family of SA modes the conditions of cooperative dynamics are fulfilled [27,28].

Examples of cooperative dynamics are shown in Fig. 7. There is no single winner as in the case of WTA competition. Six members of the mode family win or lose together. Changes in the initial values of mode amplitudes can destroy the cooperative condition (41), and different types of hexagon patterns containing cosine and sine components may appear [Fig. 7(b)]. Amplitudes of successful modes produce only symmetric stationary solutions $u(\vec{r})$ in the form of hexagonal patterns. Different symmetric solutions can be shifted in phase, which is not important for system dynamics. It is interesting that the hexagon family originates in the early development stages inside sphere ϵ_1.

For successful hexagon family formation only one initially active mode is enough. The cooperative nature of interactions within the family results in initially passive modes turning superactive [Fig. 7(a)].

Figure 7 shows sample results of a numerical investigation into the stability problem for the system of equations (33)–(37). These studies give evidence of stable solutions in the form of hexagonal structures having various orientations (i.e., different phases), and also stable rolls which can appear in the place of hexagons when initial conditions favor the roll structure. Are the hexagonal and roll form of stable solution the only possible stable solutions for this system, or perhaps are there more complicated forms similar to the society of hexagons? We cannot answer this question. The system of equations (33)–(37) could benefit from further analytical study. For the simple case of an isolated hexagon $M_f=1$ and small values of mode amplitudes, the system of hexagon equations can be performed into the mode equations, obtainable using MSA techniques [4,35]. For this case, one can use these results of the stability analysis obtained for the mode equations.

INTERACTION OF HEXAGONS

Let us follow the story of the typical six-mode "lucky" family. We will neglect the influence of sine-type modes; either the initial conditions do not include them, or they all died during the initial competition inside sphere ϵ_1 when our hexagon family first formed.

The hexagon equations describing a lucky family are derived from (33)

$$\tau\dot{a}_{m,l}^c+(1+D\kappa_m^2)a_{m,l}^c=T\{S_m Q_{m,l}^c+C_m[Q_{m,[l+1]}^c Q_{m,[l+5]}^c+Q_{m,[l+1]}^c Q_{m,[l+2]}^c+Q_{m,[l+5]}^c Q_{m,[l+4]}^c]\} \ , \tag{42}$$

where $l=0,\ldots,5$ and $T=4K(D_0^f)^2(D_0)^2$.

At the beginning of pattern formation there are many active modes inside sphere ϵ_1, so it is possible to encounter hexagons with wave vectors other than $\vec{\kappa}_m$ (recall that $\vec{\kappa}_m$ are the wave vectors at the bottom of the instability branch). Accordingly, we need to expand the previous description for pattern formation inside sphere ϵ_1 since the hexagons compete as separate units. The interactions between hexagons ($\boxed{\text{H}}\Leftrightarrow\boxed{\text{H}}$ interaction) and active modes and a hexagon ($\boxed{\text{AM}}\Leftrightarrow\boxed{\text{H}}$) must be considered (Fig. 6).

Interhexagon interactions are characterized by the heroic struggle that occurs as each hexagon attempts to confiscate its neighbor's WTA term while keeping its own. A typical $\boxed{\text{H}}\Leftrightarrow\boxed{\text{H}}$ scenario is shown in Fig. 8. Slight changes in initial conditions can switch the advantage from one hexagon [Fig. 8(a)] to the other [Fig. 8(b)]. The victorious hexagon is the one having its wave vector at the bottom of the instability branch, and generally the advantage in initial conditions as well. The result of a competition between a hexagon and an individual mode is usually obvious [Fig. 7(c)]; hexagons win this competition rather easily. The separate mode is able to kill the hexagon only if its wave vector is closer to the bottom of the instability branch, or if its initial conditions are significantly more favorable.

HYSTERESIS BEHAVIOR OF HEXAGONS

Hexagon excitation and hexagon hysteresis were investigated in [4] using multiple-scale analysis. Similar results can be obtained from the hexagon equations (42).

Assume that initial conditions hexagon modes are uniform: $a^c_{m,l}(0)=a^0$ and $a^s_{m,l}(o)=0$. Then, instead of (42), we obtain

$$\dot{a}_m+(1+D\kappa_m^2)a_m = 4KJ_0^{12}(a_m)\{\sin(\kappa_m^2 L)Q_1(a_m) +3[1-\cos(\kappa_m^2 L)]Q_1^2(a_m)\}\ , \tag{43}$$

where we have defined $a_m(t)=a^c_{m,l}(t)$.

The dependence of the stationary state solution on the parameter K is shown in Fig. 9. Inside the interval

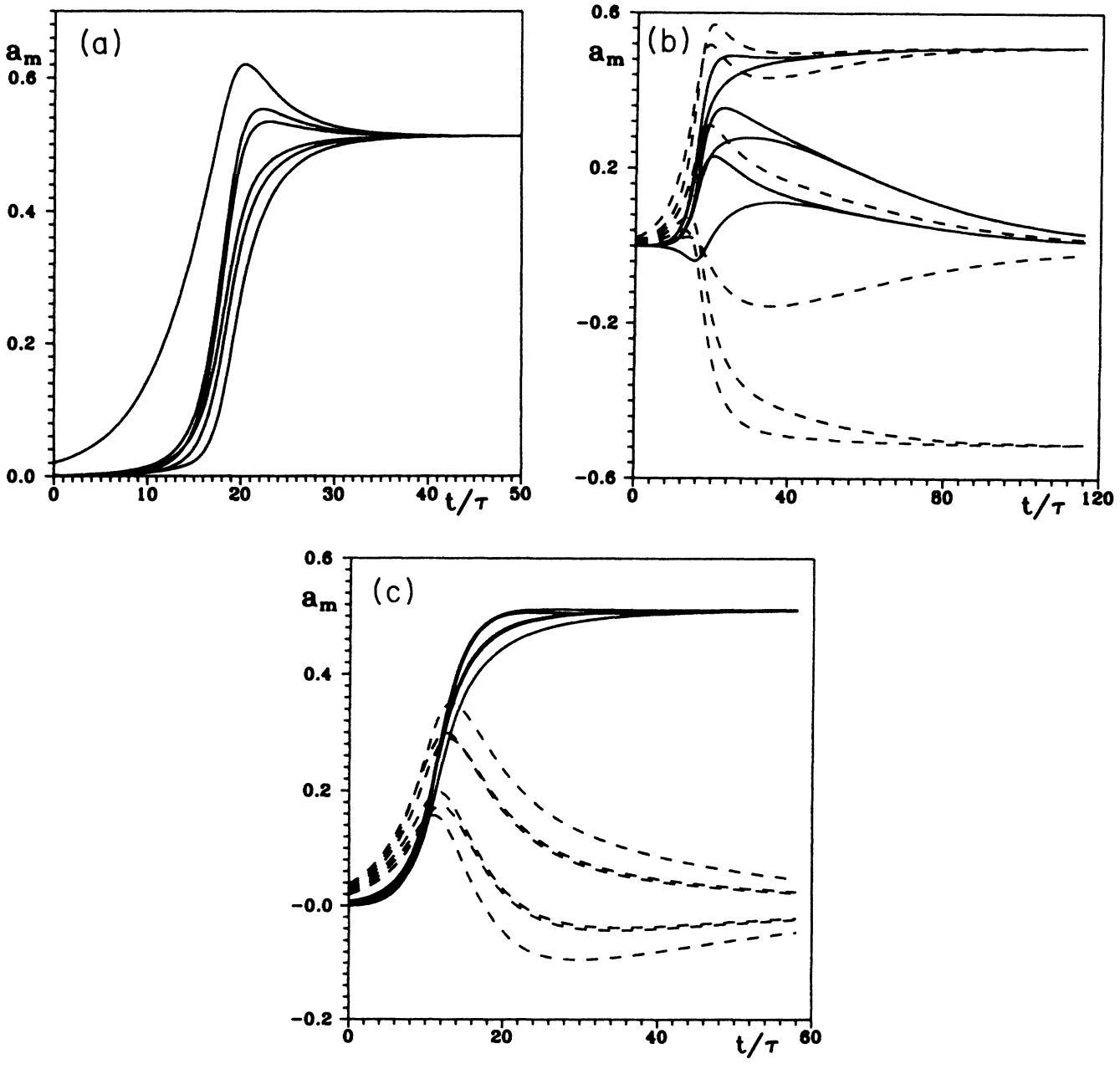

FIG. 7. Cooperative dynamics and hexagon formation ($\kappa=6.86$). Behavior of the solution to (33) for $M_f=1$, $K=-0.8$, $D=0$, $L=0.1$, $\varphi^s_{m,l}=\varphi^c_{m,l}=0$ (continuous curves correspond to cosine-type modes, dashed curves to sine-type modes). (a) $a_l^s(0)=0$ ($l=0,\ldots,5$); $a_l^c(0)=0$ ($l=0,\ldots,4$), $a_5^c(0)=0.02$. (b) $a_l^s(0)=0.005l$ ($l=0,\ldots,5$), $a_l^c(0)=0.0001l$, ($l=0,\ldots,5$). (c) Interaction between hexagons (continuous curves) and six individual SA modes with the same wave vector. Hexagon family initial conditions are $a_l^s(0)=0$, $a_l^c(0)=0.0015l$ ($l=0,\ldots,5$). Initial conditions for the SA modes are $a_m^0=0.0035m+0.02$ ($m=1,\ldots,6$).

$(K_{\rm th}^h, K_{\rm th}^m)$ are three different stationary-state solutions; only two are stable. Thus it is possible to excite hexagons in an area of stability even for control parameter values where $K < K_{\rm th}^m$. This conclusion is not contradictory since stability analysis results are valid only under the assumption that the initial amplitudes a_m^0 are within a small sphere with radius $\epsilon_0 \ll 1$. In the area $K_{\rm th}^h < K < K_{\rm th}^m$ hexagons can be excited only if the initial mode amplitudes a_m^0 are placed under the unstable branch, as shown in Fig. 9. Note that the coefficient $4K\sin(\kappa_m^2 L)$ in (43) determines the disposition of the threshold value $K_{\rm th}^m$, while $K_{\rm th}^h$ depends on the coefficient $12K[1-\cos(\kappa_m^2 L)]$. Correspondingly, variations in the wave vectors $|\vec{\kappa}_m|$ lead to shifts in the boundaries $K_{\rm th}^m$ and $K_{\rm th}^h$. Note that the shift of the threshold $K_{\rm th}^h$ is less than that for $K_{\rm th}^m$, and as a result the hysteresis area increases.

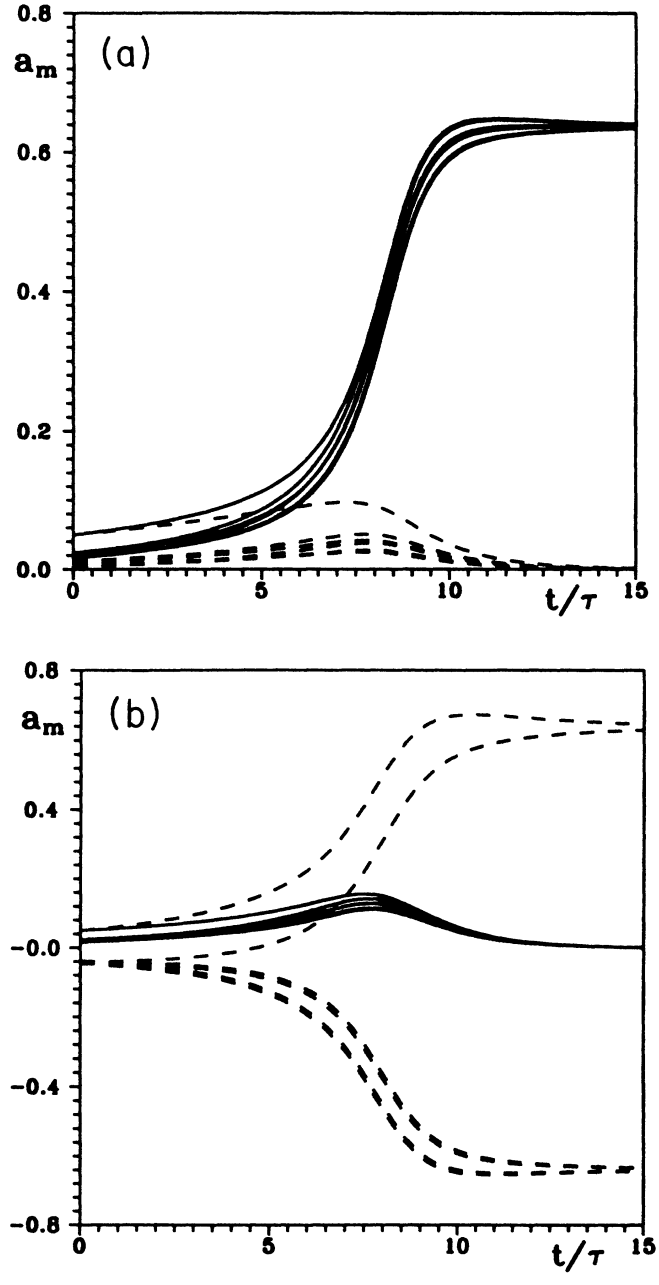

FIG. 8. Interhexagon interactions. Dependence on mode amplitudes for two hexagons with different initial conditions. Hexagon parameters are $K=0.55$, $\kappa_m=12.53$, $L=0.01$, $D=0$, $a_l^s(0)=0$ $(l=0,\ldots,5)$. (a) $a_l^c(0)=0.002(l+1)$ $(l=0,\ldots,4)$, $a_5^c=0.05$ for the first hexagon (dashed curves) and $a_l^c(0)=0.002(l+1)$ $(l=7,\ldots,11)$, $a_6^c=0.05$ for the second hexagon (solid curves). (b) $a_l^c(0)=0.002(l+1)-0.005$ $(l=0,\ldots,4)$, $a_5^c=0.05$ for the first hexagon (dashed curves) and $a_l^c(0)=0.002(l+1)$ $(l=7,\ldots,11)$, $a_6^c=0.05$ for the second hexagon (solid curves).

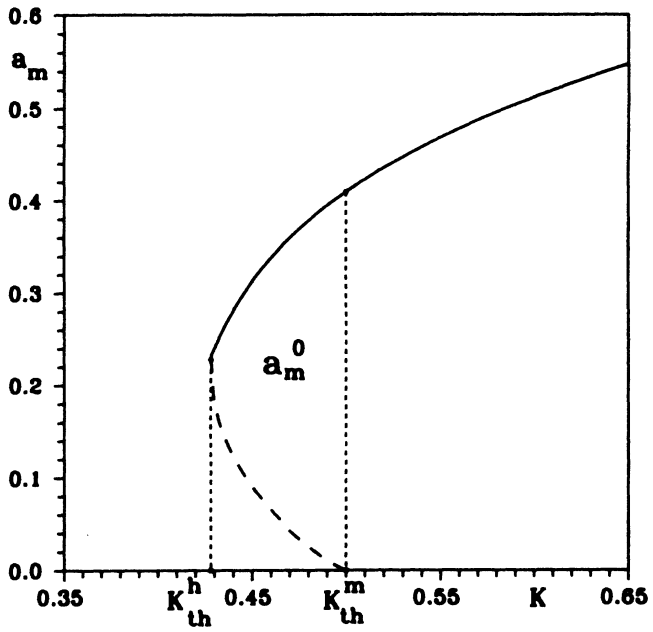

FIG. 9. Hexagon hysteresis; $\kappa_m=12.53$, $L=0.01$, $D=0$; $K>0$.

PHASE DISTORTION AND HEXAGON DISINTEGRATION

The hexagon pattern's dominant position in the field of mode dynamics appears indestructible. But all hope is not lost, as we do have yet in reserve several opportunities to annihilate the hexagon. The first is the interbranch interaction. Our "free sphere theory" does not account for feedback intensity components (29) with double wave vectors $2\vec{\kappa}_m$, as diffusion is sufficiently strong that we can keep only the most unstable branch [Fig. 2(b)]. However, for the case of minimal diffusion all branches are equally likely [Fig. 2(a)] and we need to account for components with second spatial frequencies $\vec{\nu}_m = 2\vec{\kappa}_m$. This leads to additional terms in the right-hand side of (33) for the $\vec{\nu}_m$ hexagon type. This result is coupling between two hexagons.

As the numerical simulation shows, in spite of coupling the second spatial frequencies are not excited. This is because modes with the wave vectors $\vec{\nu}_m = 2\vec{\kappa}_m$ are stable since at the bottom of the instability branch $K_{\rm th}^{2\kappa} \to \infty$.

Our last hope to destroy the hexagon is through phase distortion. Under the pressure of strong phase distortion,

hexagons begin to disintegrate [Fig. 10(b)]. As numerical simulations show, the gap between stationary-state mode amplitudes increases as phase distortion increases. The result is that in the presence of phase distortions individual SA modes and the other hexagons are not suppressed and instead survive. Amplification of phase distortions and the disintegration of hexagonal structures cause spatial modulation of the intensity; something similar to speckle modulation appears. For strong phase distortions the hexagon remains a sink in the sea of reinforced SA modes. The discontinuation of hexagon construction is accompanied by transitions between hexagons with different phases. Accordingly, spots in the intensity distribution will have short-range motions. Similar hexagon behavior occurs during transition to the turbulent regime [4]. This hexagon disintegration detracts from WTA dynamics, and, consequently, active modes independent of hexagons appear.

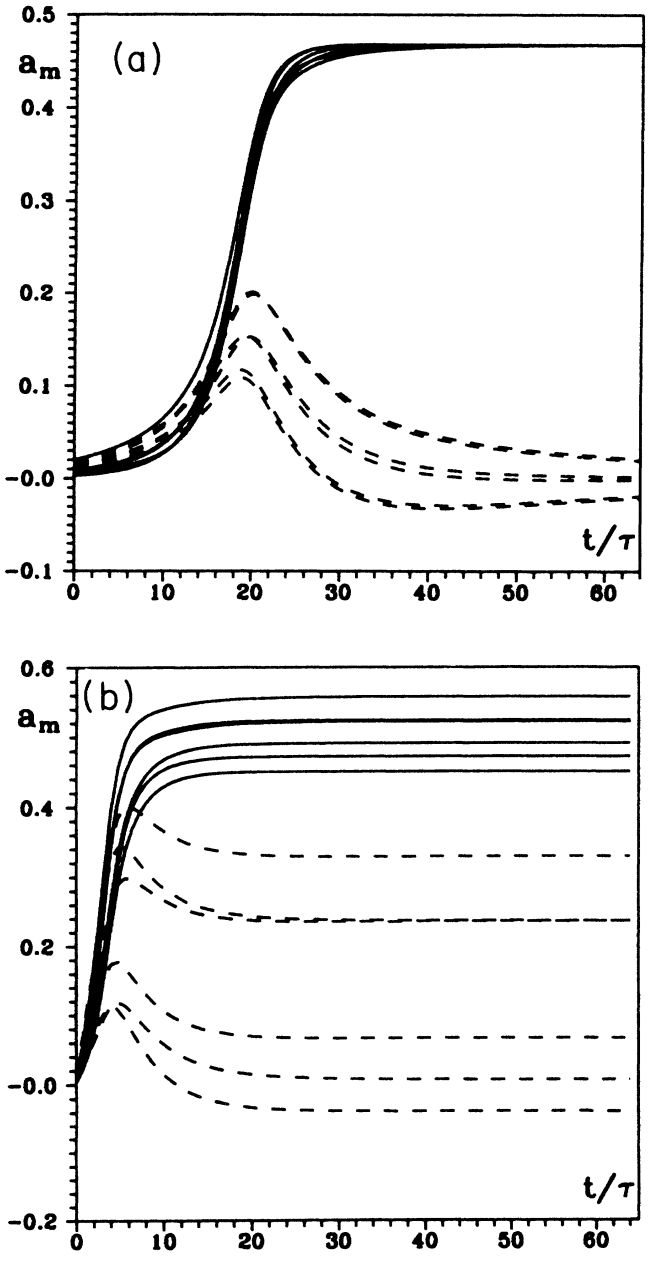

FIG. 10. Influence of phase distortions on hexagon formation; $K=0.55$, $\kappa_m=12.53$, $L=0.01$, $D=0$. (a) Without phase distortions: $\varphi_l^c=\varphi_l^s=0$, $(l=0,\ldots,5)$; $a_l^c(0)=0.0015(l+1)$ $(l=0,\ldots,4)$, $a_5^c(0)=0.02$ (solid curves), $a_l^s(0)=a_l^c(0)$ (dashed curves). (b) $\varphi_l^c=\varphi_l^s=0.01(l+1)$ $(l=0,\ldots,5)$. Initial conditions identical to case (a).

CONCLUSION

There is a classical three-step approach typically used for the study of nonlinear optical systems.

(1) Linear stability analysis, which is a reliable tool for finding potential mode candidates for the pattern formation process.

(2) Next the "guessing" of possible nonlinear modes (patterns).

(3) After carefully deciding that it is worthwhile to analyze only a selected few of these "guessed" solutions and completely ignore all other active and superactive modes, we can demonstrate the power of multiple-scale analyses or other techniques to find equations for the nonlinear mode amplitudes (in this case, hexagons).

The main point in this approach is the "guessing" of the solutions. From this point of view, a computer simulation of pattern formation helps us in this business, but not so much. In the case of rather complicated systems with long-range [32] or nonlocal [33,34] interactions, there are usually a number of nonlinear patterns with an approximately equal excitation threshold. How can we guess this?

The winning pattern depends on the interactions of patterns with themselves and with other active modes, the latter doomed to die in the process of pattern formation. This process is very sensitive to initial conditions, the influence of external perturbations, boundary conditions, etc. In this situation, neither the guessing of pattern structure nor simulation using computer are reliable methods of finding a solution.

In a Neumann-series approach we avoid merely guessing the solution by retaining the influence of all active modes. The selection of the winning pattern was based on the history of mode competition. The consequence of this competition is that the majority of modes die; this is indirectly confirmed by previous extensive numerical simulation of the Kerr-slice–feedback-mirror system [4,15]. The rolls' spatial spectrum participating in the pattern formation process becomes increasingly pure. Prior to the appearance of hexagons in this numerical simulation, the solution of the original system of equations yields an erratic combination of rolls having wave vectors located at the bottom of the instability branches [4,35].

At the same time, numerical simulations do not answer the following: Is this process of mode extinction "WTA" in character? To find out, we need to separate mode amplitudes and control WTA conditions (26) for all modes during numerical simulation. Since there are a large number of modes to consider, this analysis is a rather complicated problem.

In the Neumann's-series approach we made the transition from the actual dynamic process with a continuous spectrum of modes, towards a model having a discrete spectrum of active modes $\vec{k}_m$. What is the destiny of modes with wave vectors $\vec{k}_m+\vec{\delta}$ located in the small vicinity of $\vec{k}_m$? In our approach we ignore these modes.

In justification we offer the following. Formally, we could include in the model a large number of wave vectors (modes) located close to the superactive mode wave vectors. This would mean that a great number of additional hexagonal families and superactive modes would appear and take part in the competition. Because all of these hexagons have almost the same excitation threshold and highly similar initial conditions, the competition process will develop slowly. Instead of just one single hexagon family, we now have an envelope of hexagon families that will exist a rather long time. Due to competition the width of this envelope in $\vec{k}$ space decreases, forming in the limit one hexagon family containing discrete $\vec{k}$ vectors.

This is true only for the case of a Kerr slice with unlimited aperture size. With numerical simulation this case is obtained by using periodic boundary conditions. In real experiments the spectrum width will stop decreasing, due to the influence of boundary conditions [36,18]; finite systems cannot have discrete spectra.

Boundary conditions have effects other than simply causing imperfections in hexagons. We ignore this effect in our approach. If the distance $(\lambda L)^{1/2}$ under the influence of diffraction from the aperture is on the order of the aperture size a, that is, $L/(ka^2)=1/2\pi$, we have the new situation of the a system with long-range interactions. In fact, the influence of boundary conditions can cause radical changes in dynamics even if $(\lambda L)^{1/2}$ is significantly less than a. This reason, along with the presence of phase distortions, yields the result that in actual experiments hexagons appear less often than other patterns such as polygons, spots, etc.

The problem of boundary conditions, or, in a more general statement, the problem of pattern formation in systems having long-range or global interactions, is very interesting and important [38,15]. Hopefully, future studies will show if it is advantageous to apply the Neumann-series approach to this problem. The answer to this question will perhaps depend on the level of rigor in formulas derived.

ACKNOWLEDGMENTS

We are grateful to L. A. Lugiato and F. T. Arecchi for helpful discussions and to J. Ricklin for many useful suggestions and comments. This work was supported by a Royal Society Grant No. 1265/92.

[1] G. Giusfredi, J. F. Valley, G. Khitrova, and H. M. Gibbs, J. Opt. Soc. Am. A **5**, 1181 (1988).
[2] W. J. Firth, J. Mod. Opt. **37**, 151 (1990).
[3] R. Macdonald and H. J. Eichler, Opt. Commun. **89**, 289 (1992).
[4] G. D'Alessandro and W. J. Firth, Phys. Rev. A **46**, 537 (1992).
[5] G. Grynberg, Opt. Commun. **66**, 321 (1988).
[6] G. Grynberg, E. Le Bihan, P. Verkerk, P. Simoneau, J. R. R. Leite, D. Bloch, S. Le Boiteux, and M. Ducloy, Opt. Commun. **67**, 363 (1988).
[7] J. Y. Courtois and G. Grynberg, Opt. Commun. **87**, 186 (1992).
[8] H. M. Gibbs, *Optical Bistability: Controlling Light with Light* (Academic, New York, 1985).
[9] M. A. Vorontsov and K. V. Shishakov, J. Opt. Soc. Am. B **9**, 71 (1992).
[10] M. A. Vorontsov, Proc. Soc. Photo-Opt. Instrum. Eng., **1402**, 116 (1991).
[11] S. A. Akhmanov, M. A. Vorontsov, V. Yu. Ivanov, A. V. Larichev, and N. I. Zheleznykh, J. Opt. Soc. Am. B **9**, 78 (1992).
[12] N. B. Abraham and W. J. Firth, J. Opt. Soc. Am. B **7**, 951 (1990).
[13] L. A. Lugiato, G. L. Oppo, J. R. Tredicce, L. M. Narducci, and M. A. Pernigo, J. Opt. Soc. Am. B **7**, 1019 (1990).
[14] F. T. Arecchi, Physica D **51**, 450 (1991).
[15] F. Papoff, G. D'Alessandro, G.-L. Oppo, and W. J. Firth, Phys. Rev. A **48**, 634 (1993).
[16] M. A. Vorontsov, Kvant. Elektron (Moscow) **20**, 319 (1993).
[17] E. V. Degtyarev and M. A. Vorontsov, Mol. Cryst. Liq. Cryst. Sci. Technol. Sec B: Nonlinear Opt. **3**, 295 (1992).
[18] M. Tamburrini, M. Bonavita, S. Wabnitz, and E. Santamato, Opt. Lett. **18**, 855 (1993).
[19] A. C. Newell, *The Dynamics and Analysis of Patterns,* Lectures in The Sciences of Complexity, SFI Studies in the Sciences of Complexity (Addison-Wesley, Reading, MA, 1989).
[20] B. S. Kerner and V. V. Osipov, Usp. Fiz. Nauk **160**, 3 (1990) [Sov. Phys. Usp. **33**, 1 (1990)].
[21] J. E. Bjorkholm, P. W. Smith, W. J. Tomlinson, and E. A. Kaplan, Opt. Lett. **6**, 345 (1981).
[22] M. A. Vorontsov, A. V. Koriabin, and V. I. Shmalhauzen, Controlling Optical Systems (Nauka, Moscow, 1988).
[23] W. J. Firth and M. A. Vorontsov, J. Mod. Opt. **40**, 1841 (1993).
[24] G. N. Watson, *Theory of Bessel Functions* (Cambridge University Press, Cambridge, England, 1962).
[25] N. G. Iroshnikov and M. A. Vorontsov, in *Essay in Nonlinear Optics: in Memorium of Serge Akhmanov,* edited by H. Walther and N. Koroteev (IOP, London, 1992).
[26] H. Haken, *Advanced Synergetics* (Springer-Verlag, New York, 1987).
[27] S. Grossberg, Neural Networks **1**, 17 (1988).
[28] M. W. Hirsch, SIAM J. Math. Anal. **16**, 423 (1985).
[29] J. W. Goodman, *Introduction to Fourier Optics* (McGraw-Hill, San Francisco, 1968), Vol. 42.
[30] M. A. Vorontsov (unpublished).
[31] *Parallel Distributed Processing,* edited by D. Rumelhart and J. McClelland (MIT Press, Cambridge, MA, 1986).
[32] M. C. Cross and P. C. Hohenberg, Rev. Mod. Phys. **65**, 851 (1993).
[33] M. A. Vorontsov and A. V. Larichev, Proc. Soc. Photo-

Opt. Instrum. Eng. **1409**, 260 (1991).
[34] H. Adachihara and H. Faid, J. Opt. Soc. Am. B **10**, 1242 (1993).
[35] S. Ciliberto, P. Coullet, J. Lega, E. Pampaloni, and C. Perez-Garcia, Phys. Rev. Lett. **65**, 2370 (1990).
[36] M. Kreuzer, W. Balzer, and T. Tschudi, Opt. Lett. **29**, 579 (1990).
[37] J. V. Moloney and A. C. Newell, *Nonlinear Optics* (Addison-Wesley, Redwood City, CA, 1991).

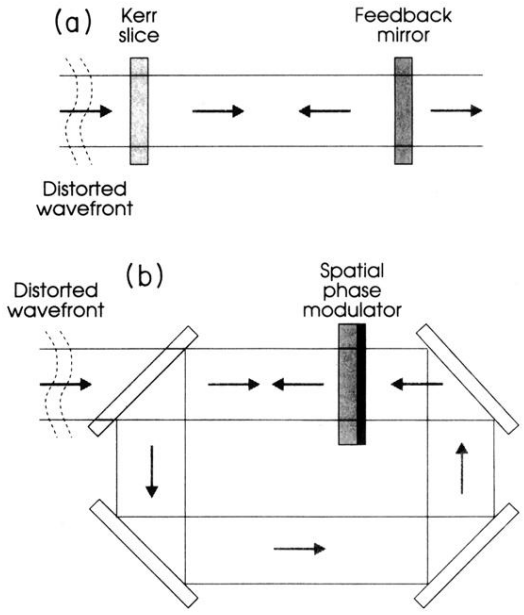

FIG. 1. Two optical systems which are equivalent in terms of the present analysis: (a) Kerr slice with feedback mirror; (b) nonlinear passive resonator controlled by a spatial phase modulator driven by light through a 2D feedback loop.